OPTICAL REMOTE SENSING FOR GLACIER MONITORING WITH RESPECT TO DIFFERENT SNOW AND ICE TYPES: A CASE STUDY FOR THE SOUTHERN PATAGONIAN ICEFIELD

Janine Florath[1], *Sina Keller*[1], *Guido Staub*[2], *Martin Weinmann*[1]

[1] Institute of Photogrammetry and Remote Sensing, Karlsruhe Institute of Technology (KIT), Germany
[2] Department for Geodetic Sciences and Geomatics, University of Concepción, Chile

ABSTRACT

In this paper, we evaluate the possibility of using optical remote sensing techniques to survey remote glacier areas, where conventional surveying techniques are difficult to carry out. The extent of different spectral classes on the Tyndall glacier area in the Southern Patagonian icefield, Chile, is evaluated through classification with respect to five different snow and ice types on the surface of the glacier. Different classification approaches are tested for their eligibility to identify these snow and ice types. As no labeled data is available for the investigated remote area, a novel method is tested to obtain labeled Sentinel-2 compliant data from theoretical spectral reflectance curves. The achieved classification results show that all examined classification approaches are suitable for detecting different spectral snow and ice classes on the glacier surface.

Index Terms— Remote Sensing, Glacier Monitoring, Snow Mapping, Classification, Multi-/Hyperspectral Data

1. INTRODUCTION

Remote sensing surveying techniques are nowadays widely used for various applications. One of the primary purposes is to map areas with different land cover types. These techniques allow the overview of a larger area than conventional, terrestrial survey methods in a shorter time and with less effort. A remote area is studied in this work, which would cost an inefficiently high effort to survey with terrestrial methods.

The Campo de Hielo Patagónico Sur (CHPS) is an icefield in Southern Patagonia between Chile and Argentina. It is still poorly known as research in this remote area, in general, is challenging. Previous studies focus on the development of the glacier extent and mass balance [1, 2]. Apart from only the extent, the knowledge of the snow and ice cover types of the glaciers is significant, as the variability of seasonal snow cover is an essential parameter in the climate system.

This study's main objective is to carry out an automatic classification concerning different snow and ice types on a glacier surface using Sentinel-2 data to benefit from the high resolution, as shown in Fig. 1. As no reference data is available for different snow and ice cover types in the investigated area, suitable reference data is obtained from theoretical knowledge [3]. More specifically, labeled Sentinel-2-like data are simulated by reducing from densely sampled spectral reflectance curves representing different snow and ice cover types to spectral reflectance curves representing information on Sentinel-2 bands only. The latter corresponds to the transfer from hyperspectral data to Sentinel-2-like data [4, 5, 6]. On this basis, four classification approaches are investigated: two unsupervised approaches, the k-means clustering and a rule-based classification via snow and ice indices, and two supervised approaches, the Linear Discriminant Analysis (LDA) and the Random Forest [7] (RF) classifiers.

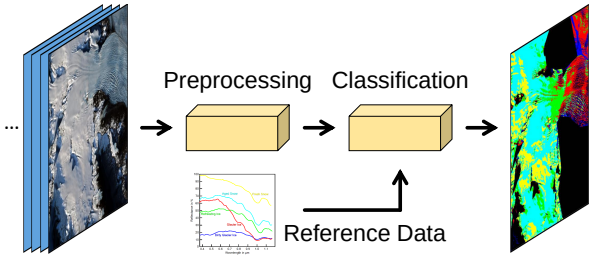

Fig. 1: Overview of the applied glacier monitoring approach.

2. RELATED WORK

Multitemporal analysis of a glacier concerning different snow and ice types is relevant to detect changes in the glacier's surface composition. Different classes influence the glacier's behavior (melting or refreezing on the glacier) in different ways.

The knowledge of the snow-covered area facilitates a diversity of applications, for example, water resource management. While snow cover plays an essential role in general, snow cover on a glacier is particularly of interest: Deep snow cover on the glacier keeps glacier temperature colder and therefore prevents more melting and water run-off. In [8], different snow seasons with different average snow depths are evaluated. A deeper snow depth causes a delay in the

snow cover time to reach isothermal conditions, which allows the snow cover on the glacier to persist longer. The separation into the classes of new and aged snow allows statements about the snow wetness, one of the main physical properties of snow. Snow wetness accordingly allows statements about the location of zones of accumulation areas on the glacier.

Besides the snow cover, different ice types might also strongly influence the behavior of a glacier. On the one hand, a classification concerning the class *dirty glacier ice* allows reasoning about the extent of debris cover on the glacier surface. The influence of debris cover on the processes on and within the glacier is described in [9]. There, achieved results indicate that ice with debris cover reveals lower melting rates than clean ice. Even a small debris cover thickness of only $1\,\mathrm{cm}$ to $2\,\mathrm{cm}$ reduces ice melting. Moreover, the study suggests that a thinning glacier naturally becomes debris-covered over the ablation area as more debris from the sides of the glacier spreads on it. The debris cover on the ice naturally reduces the rate of ice loss. On the other hand, separation of an extra class for *refreezing ice* is relevant, as the refreezing of meltwater may prevent immediate run-off of meltwater and therefore influence glacier ablation [10].

In related work, the definition of snow and ice types varies a lot [11], and there is no general definition. A large-scale analysis of glaciers for snow/ice cover classes like the ones mentioned before may be achieved by using multispectral satellite imagery, as there is a large difference in snow and ice reflectance in the visible, near-infrared (NIR) and shortwave infrared (SWIR) regions of the spectrum for these classes. For instance, in the visible part of the spectrum, the reflectance is very high for freshly fallen pure snow, while it decreases with the age of the snow and given impurities [3]. For each class, a relatively unique shape of the spectral signature is given with characteristic spectral differences across the spectrum. This shape represents the basis for most multispectral glacier mapping applications [12] and can be treated in analogy to semantic segmentation of remote sensing data in general [13, 14], given representative and sufficient training data.

3. METHODOLOGY

After focusing on the classes taken into consideration for this work (Section 3.1), we explain how reference data are created for the classification task (Section 3.2). Subsequently, we describe the performed data preprocessing (Section 3.3) and the applied classification approaches (Section 3.4).

3.1. Class Definition

Several physical properties define a type of snow or ice. In this work, only the characteristics that change the spectral signature of the actual snow/ice type can be detected due to the use of multispectral satellite imagery. Hence, only snow and ice types that can be separated accordingly are considered:

- *Glacier ice*: ice, which forms where the accumulation of snow and ice exceeds ablation. Different geological features need to be met to allow the formation of a glacier. As snow falls and is compressed and contained air is squeezed, the snow slowly turns into glacier ice. Compared to refreezing ice, glacier ice exists in the lower parts of the glacier and is older.
- *Refreezing ice*: superimposed ice and blue ice, which occurs when snow falls on an already existing glacier and is compressed and becomes part of the glacier in newer years of the glacier's existence.
- *Dirty ice*: dirty glacier ice is basically glacier ice that is mixed with impurities, mostly debris. The term debris here is taken to include all rock materials lying on the glacier or adjacent to the glacier, where it encounters non-glacier material on its borders in the adjoining valley (mostly bare rock/soil). Even small impurities of soil can cause a different spectral reflectance of the ice and, therefore, a classification into the class of dirty ice.
- *Aged snow*: aged snow is characterized by being melted and refrozen due to changes in incident solar radiation and temperature. Therefore, it contains a higher water content than fresh snow and more impurities due to a long time being on the ground. It has a lower reflectance value.
- *Fresh snow*: newly fallen snow shows contrary properties to aged snow. It has lower water content and contains fewer impurities, leading to a higher reflectance.

3.2. Generation of Reference Data

Suitable reference data are obtained from theoretical knowledge in the form of given, densely sampled spectral signatures for either class according to [3], as shown in Fig. 2. As for the classification of full scenes of the glaciers, the class *water* is added, labeled reference data are also necessary for this class and generated accordingly from a given spectral reflectance curve. On that data basis, interpolation is applied to obtain the spectral reflectance curves (SRCs) with values for steps of $1\,\mathrm{nm}$ in wavelength. Subsequently, the spectral response functions (SRFs) of the Sentinel-2 multispectral instrument and the derived SRCs are used to calculate the weighted mean of the reflectance values per class per band.

As, for the given classes, the created dataset contains only five samples, which does not reflect the whole variance of spectral values that a spectral class might comprise, the creation of a bigger dataset is necessary. This creation is obtained by applying the Nearest-Neighbour (NN) algorithm. To obtain a non-committed result in the evaluation of classification results, training data (Training Areas = TAs) and test data (Test Areas = TEs) are created: independent Regions Of Interest (ROIs) are chosen on the glacier area, manually selected based on the data created through the NN algorithm.

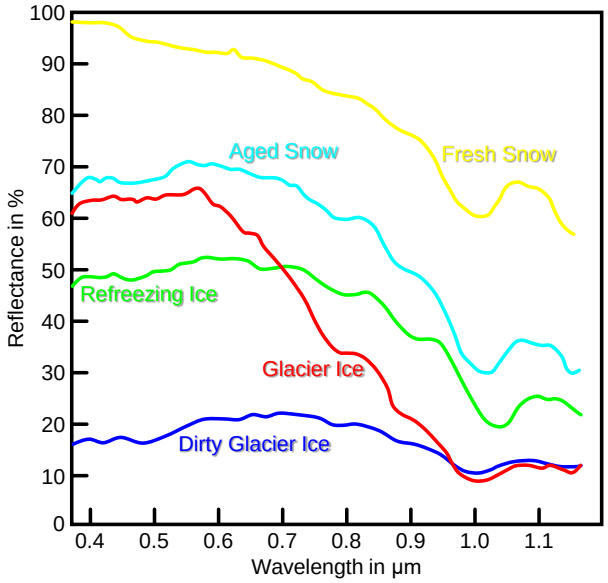

Fig. 2: Spectral signatures for snow and ice classes, cf. [3].

3.3. Preprocessing

Some preprocessing steps are required to work with the available satellite data. These steps address an atmospheric correction via the Sen2Cor software, where the correction is performed according to [15]. Furthermore, we apply an image enhancement for each band of the multispectral imagery by mapping values that lie below or above the boundary $1\,\%$-percentile to the percentile's value and subsequently scaling the resulting values for each band to a range of $0\,\%$ to $100\,\%$. Finally, ROIs are selected for the following analyses. As only the glacier itself is considered in this study, while the area surrounding the glacier is not of particular interest, a corresponding mask as well as a shadow mask are created.

3.4. Classification

We investigate four classification approaches. These comprise two unsupervised approaches represented by k-means clustering and a rule-based classification, and two supervised approaches represented by LDA and RF classifiers.

For the k-means clustering, k is selected as the number of centroids needed for the given dataset. After clustering, the obtained clusters are assigned to the pre-defined classes based on their Euclidean distance to respective reference spectra to compare with the results of other methods.

For the rule-based classification, we follow [16], where different spectral indices are used to separate between different snow cover classes. These indices comprise the Normalized Difference Snow Index (NDSI), the Normalized Difference Glacier Index (NDGI), and the Normalized Difference Snow Ice Index (NDSII). After calculating these indices, thresholds are applied to separate the data for classes defined in [16]. In this context, suitable thresholds need to be found and – as the thresholds may vary with different sensors and seasons and are even scene-dependent – they are chosen experimentally. Furthermore, we adapt the class definitions for our pre-defined classes to compare the results with those achieved with other considered classification approaches.

For the LDA classifier, Gaussian distribution parameters are estimated for each class during the training, assuming that each of the classes is characterized by a mean vector μ_i and the same covariance matrix Σ. A new sample can then be classified by maximizing the likelihood of that sample.

For the RF classifier [7], the training consists of generating an ensemble of randomly different decision trees via bootstrap aggregating ("bagging"). A pre-defined number of weak learners represented by decision trees are trained independently from each other on subsets of the training data, which are randomly drawn with replacement. For a new sample to be classified, each decision tree casts a vote for one of the defined classes and considering the majority vote across the individual votes allows for a robust class prediction.

4. EXPERIMENTAL RESULTS AND DISCUSSION

After focusing on the study area (Section 4.1), we proceed with analyzing the quality of the reference data (Section 4.2) and the achieved classification results (Section 4.3).

4.1. Study Area

The extent of the whole Patagonian icefield (Campo de Hielo Patagónico Sur; CHPS), which stretches for about $350\,\mathrm{km}$ [17], is too large to undertake a study of precise snow/ice type classification. Hence, in this work, only a subset of the Torres del Paine National Park is considered, as it presents a great physical, climatic and biological diversity. This park comprises the Grey, Tyndall and Dickson glaciers, which are some of the main 20 glaciers in the CHPS. Representatively for these three glaciers that are influenced by the same climatic and weather changes, the snow and ice cover development of the Tyndall glacier is studied in the scope of this work. This glacier is one of the largest glaciers in the Southern Patagonian icefield, with an approximate length of $32\,\mathrm{km}$.

4.2. Quality Assessment for the Derived Reference Data

The quality of the generated reference data is evaluated per class by comparing obtained reflectance values with theoretical spectral reflectance curves. For each band, the mean values correspond well with the theoretical curves (Fig. 2) for most of the classes, and the standard deviations are quite similar for all bands in all classes, with about $5\,\%$ to $10\,\%$. Some outliers occur for Band 1 for the class of *dirty glacier ice*, and the main mixing of the values occurs in the Bands 1-3 for the classes *aged snow*, *glacier ice*, and *refreezing ice*.

Table 1: Comparison of the results achieved with the applied classification approaches (Clust: Clustering with $k = 8$; RBC: Rule-based classification) with values in %.

Metric	Clust	RBC	LDA	**RF**
OA	84.70	90.98	97.26	**97.49**
κ-index	79.73	84.00	96.38	**96.68**
mean F_1-score	83.37	82.40	96.39	**96.70**
Recall mean	82.05	79.09	96.35	**96.65**
Precision mean	84.73	86.00	96.43	**96.75**
Recall min	53.40	32.18	89.70	**89.77**
Recall max	**100.00**	99.47	**100.00**	**100.00**
Precision min	57.97	74.33	92.12	**93.01**
Precision max	**100.00**	99.18	**100.00**	**100.00**

However, this approach has some drawbacks: First of all, the generated reflectance curves representing theoretical knowledge of reflectance properties for individual classes are not specifically chosen for the considered study area. Reflectance values for certain snow and ice classes might vary depending on higher impurity contents in snow/ice or for other reasons. Furthermore, the read-off from the reflectance curves to data points might not be that accurate. Such slight deviations from the underlying theoretical reflectance curves might, however, be an advantage, as it may improve the generalization of the used spectral reflectance curves.

4.3. Classification Results

We apply the k-means clustering for different values of k. A subsequently performed in-depth analysis reveals that a selection of k=8 delivers good results for the assignment of cluster centers to the considered snow/ice classes, with an overall accuracy (OA) of 84.70% as displayed in Table 1.

For the rule-based classification described in Section 3.4, suitable thresholds need to be found for an appropriate separation with respect to the different classes. This separation is achieved by considering histograms of the indices and successively selecting thresholds that are useful for separating classes across several steps. The assumption of comparability of the thus defined classes to the pre-defined classes is necessary. It can be made, as the obtained results from the rule-based method show similar structures of snow/ice classes as the reference data. The NN algorithm is used to finally assign the classes obtained from the rule-based classification to those classes given with the generated reference data. The achieved classification results reveal a high quality indicated by an OA of 90.98%, while the κ-index and the mean F_1-score across classes are given with 84.00% and 82.40%, respectively. However, the high OA should be considered with caution. In this case, the results are biased, as a separation between *fresh snow* and *aged snow* is not taken into account due to the original class definition based on the spectral indices.

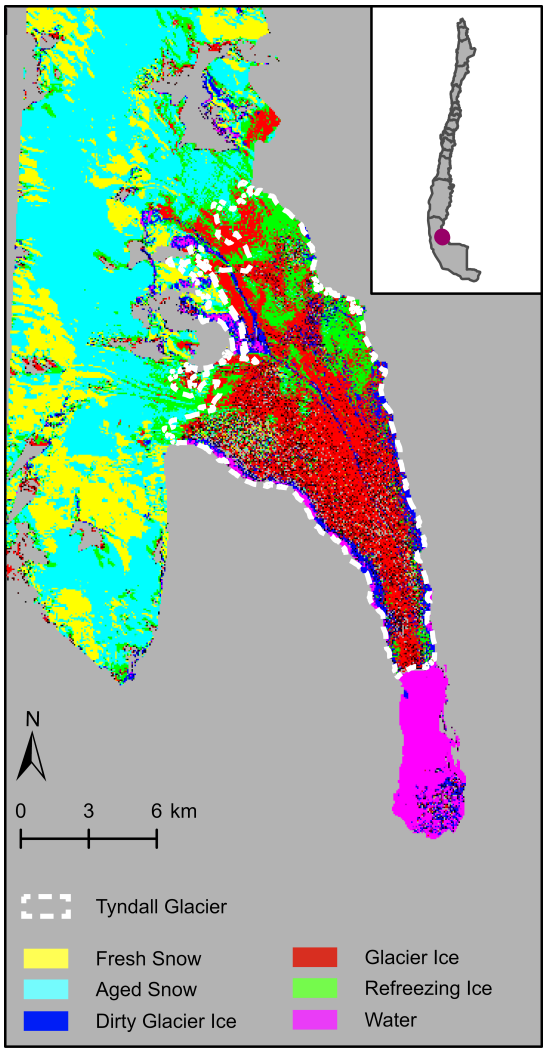

Fig. 3: Visualization of the study area in Chile and the classification results achieved with the applied RF approach.

These two classes are considered and evaluated as one. The confusion between those classes is not evident in the OA but indicated with a low minimum recall of 32.18%.

The results obtained by the LDA classifier have a rather high accuracy, with all considered evaluation metrics being in the range of about 90-100%. Class-wise evaluation reveals that the class *refreezing ice* has the lowest recall and precision, which reveals that it is a little more difficult for the algorithm to classify this class compared to the others.

For the RF classifier, the internal parameters are selected based on a grid search, showing the best results for 100 decision trees, a maximum tree depth of 20, and a minimum number of 5 data points allowed at child nodes for a further split. The achieved results reveal the highest accuracy among the tested methods, with an OA of 97.49%. Classification results for this approach are displayed in Fig. 3 for the date of 08/05/2019 together with the glacier outline of 04/02/2017.

5. CONCLUSIONS

In this work, we focused on the classification of the surface of a glacier in the region of the Torres del Paine National Park in Southern Chile with respect to different snow and ice classes. While the use of multispectral data generally allows for such large-scale analyses, we faced a major challenge because no reference data was available, which could be used for training a supervised classification approach towards separating the pre-defined classes. We addressed this challenge by generating suitable reference data from theoretical knowledge in the form of given, densely sampled spectral signatures for either class. This can be considered as interpretation of theoretical spectral signatures in terms of hyperspectral data that are subsequently transformed into multispectral data. From the obtained primary data, further labeled reference data points are aggregated by applying the NN algorithm to create a larger dataset. On this basis, the performance of four different classification approaches was evaluated: (a) k-means clustering, (b) rule-based classification via snow and ice indices, (c) LDA classifier, and (d) RF classifier. The achieved results for classification with respect to snow and ice types on the Tyndall glacier are relatively good for all tested classification approaches, with the RF representing the best-performing approach. A major limitation of the presented work is common with other optical remote sensing techniques, as multispectral Sentinel-2 data is only appropriate for cloud-free scenes. Nevertheless, this work serves as a good basis for future investigations, which will focus on a multitemporal analysis addressing the development of the glacier over time.

6. REFERENCES

[1] A. Rivera and G. Casassa, "Ice elevation, areal, and frontal changes of glaciers from National Park Torres del Paine, Southern Patagonia Icefield," *Arctic, Antarctic, and Alpine Research*, vol. 36(4), pp. 379–389, 2004.

[2] N. Sáez, G. Staub, and R. Abarca-del-Río, "Monitoring glacier retreat in the Chilean Southern Patagonian Ice Field," in *Proc. IGARSS*. IEEE, 2019, pp. 4169–4171.

[3] A.J. Dietz, C. Kuenzer, U. Gessner, and S. Dech, "Remote sensing of snow–A review of available methods," *Int. J. Remote Sens.*, vol. 33(13), pp. 4094–4134, 2012.

[4] F. Thonfeld, H. Feilhauer, and G. Menz, "Simulation of Sentinel-2 images from hyperspectral data," in *Proc. Sentinel-2 Preparatory Symposium*, 2012.

[5] M. Weinmann, P.M. Maier, J. Florath, and U. Weidner, "Investigations on the potential of hyperspectral and Sentinel-2 data for land-cover / land-use classification," *ISPRS Ann. Photogramm. Remote Sens. Spat. Inf. Sci.*, vol. IV-1, pp. 155–162, 2018.

[6] P.M. Maier and S. Keller, "Application of different simulated spectral data and machine learning to estimate the chlorophyll a concentration of several inland waters," in *Proc. WHISPERS*. IEEE, 2019, pp. 1–5.

[7] L. Breiman, "Random forests," *Mach. Learn.*, vol. 45(1), pp. 5–32, 2001.

[8] M. Maggioni, M. Freppaz, P. Piccini, M.W. Williams, and E. Zanini, "Snow cover effects on glacier ice surface temperature," *Arctic, Antarctic, and Alpine Research*, vol. 41(3), pp. 323–329, 2009.

[9] B. Pratap, D.P. Dobhal, M. Mehta, and R. Bhambri, "Influence of debris cover and altitude on glacier surface melting: a case study on Dokriani Glacier, central Himalaya, India," *Annals of Glaciology*, vol. 56(70), pp. 9–16, 2015.

[10] A.P. Wright, J.L. Wadham, M.J. Siegert, A. Luckman, J. Kohler, and A.M. Nuttall, "Modeling the refreezing of meltwater as superimposed ice on a high Arctic glacier: a comparison of approaches," *J. Geophys. Res.: Earth Surface*, vol. 112(F4), pp. 1–14, 2007.

[11] C. Fierz, R.L. Armstrong, Y. Durand, P. Etchevers, E. Greene, D.M. McClung, K. Nishimura, P.K. Satyawali, and S.A. Sokratov, *The International Classification for Seasonal Snow on the Ground*, UNESCO/IHP, 2009.

[12] A. Kääb, T. Bolch, K. Casey, T. Heid, J.S. Kargel, G.J. Leonard, F. Paul, and B.H. Raup, "Glacier mapping and monitoring using multispectral data," *Global Land Ice Measurements from Space*, pp. 75–112, 2014.

[13] X.X. Zhu, D. Tuia, L. Mou, G. Xia, L. Zhang, F. Xu, and F. Fraundorfer, "Deep learning in remote sensing: a comprehensive review and list of resources," *IEEE Geosci. Remote Sens. Mag.*, vol. 5(4), pp. 8–36, 2017.

[14] M. Schmitt, J. Prexl, P. Ebel, L. Liebel, and X.X. Zhu, "Weakly supervised semantic segmentation of satellite images for land cover mapping – challenges and opportunities," *ISPRS Ann. Photogramm. Remote Sens. Spat. Inf. Sci.*, vol. V-3-2020, pp. 795–802, 2020.

[15] U. Müller-Wilm, *Sentinel-2 MSI – Level-2A Prototype Processor Installation and User Manual*, Telespazio VEGA Deutschland GmbH, 2016.

[16] A.K. Keshri, A. Shukla, and R.P. Gupta, "ASTER ratio indices for supraglacial terrain mapping," *Int. J. Remote Sens.*, vol. 30(2), pp. 519–524, 2009.

[17] H. De Angelis, F. Rau, and P. Skvarca, "Snow zonation on Hielo Patagónico Sur, Southern Patagonia, derived from Landsat 5 TM data," *Global and Planetary Change*, vol. 59(1-4), pp. 149–158, 2007.